Image Registration Techniques Alter Image Properties in fMRI

by

Kevin K. Liu

A essay submitted to the Faculty of the Graduate School,
Marquette University,
In Partial Fulfillment of the requirements for
The Degree of Master of Science

Milwaukee, Wisconsin

April 2016

Abstract
Image Registration Techniques Alter Image Properties in fMRI

Kevin K. Liu

Marquette University, 2016

In functional magnetic resonance imaging (fMRI), complex valued data is collected, reconstructed, and processed before it becomes a recognizable image. Each step is important in creating quality images, image processing specifically enhances the overall or a particular aspect of an image. A particularly important process is image registration, the alignment of two or more images through geometric transformations. Registration is not unique to medical imaging, it is complex and a challenging computational problem. Within fMRI it is used for motion correction and spatial normalization. It has been shown in recent studies that some image processing operations can induce artificial correlation of non-biological origins between voxels. Quantifying any potentially induced correlation from image registration can allow for future development of statistical models that greatly improve the accuracy and reliability of fMRI studies.

Acknowledgements

Kevin K Liu

I would like to express my sincere gratitude to my advisor, Dr. Rowe, who introduced to the field of fMRI and provided his invaluable time and guidance.

Table of Contents

Chapters

1. Introduction

Functional magnetic resonance imaging (fMRI) can find active parts of the brain by observing changes in the blood oxygenation level dependent (BOLD) signal. The complex-valued signal is acquired in the spatial frequency domain and reconstructed with a 2-D discrete inverse Fourier Transform.

Aside from reconstruction, multiple image processing steps are implemented for different reasons. One reason being that it is impossible to obtain perfectly aligned images, both inter-subject and intra-subject studies produce some degree of misalignment between images. Inter-subject images are prone to the variation in size and physical features between subjects. Whereas intra-subject images are prone to any kind of motion, even something as regular as breathing. Both of these images need to be aligned before any meaningful analysis can be performed. Registration is the process which addresses these issues, making it a very important step in fMRI.

i. Research Problem

Image processing is a crucial step to improving the quality of reconstructed MRI data, but spatial and temporal correlation of no biological origin can be induced. Both the degree and structure of the induced correlation varies across different image processing techniques. Other statistical properties of an image can be changed as well. Since fMRI analysis is conducted after multiple steps of images processing and reconstruction, the reliability of analysis results can be compromised by induced correlations. In addition, when multiple image processing operations are performed, the degree and structure of the induced correlation is changed.

Quantification of induced correlations is vital to refining fMRI analysis. Because image registration has become an expansive topic with many approaches, only the popular methods of

registration will be addressed. The aim of this project is to both show and quantify any induced correlation from image registration.

2. Background

i. Linear Framework for Data Reconstruction

Linear image processing techniques can be represented as a linear matrix operator which can perform the process as a single matrix multiplication. When complex-valued fMRI data is collected in the spatial frequency domain, *k*-space, it is reconstructed into a recognizable image using a discrete inverse Fourier transformation. A complex-valued matrix application of the discrete inverse Fourier transformation is used to develop a one-to-one relationship between *k*-space data and reconstructed voxel measurements, Eq. 1.

$$\Omega = \begin{bmatrix} \Omega_R & -\Omega_I \\ \Omega_I & \Omega_R \end{bmatrix}, \text{ where } \begin{matrix} \Omega_R = [(\Omega_{yR} \otimes \Omega_{xR}) - (\Omega_{yI} \otimes \Omega_{xI})] \\ \Omega_I = [(\Omega_{yR} \otimes \Omega_{xI}) - (\Omega_{yI} \otimes \Omega_{xR})] \end{matrix} \quad (1)$$

If the discrete inverse Fourier transformation is represented as a matrix operator then the reconstruction can be performed as a matrix multiplication [9].

$$v = \Omega f \quad (2)$$

Where matrix Ω is a discrete inverse Fourier transformation matrix operator, f is a vector of observed values, and v is the reconstructed complex-valued data.

ii. Computing Correlation

By developing matrix operator representations, the theoretical induced correlation can be quantified. Although this could also be accomplished through simulation, a matrix operator is superior in both computational efficiency and accuracy. Given Eq. 2, if the original vector f has a known mean and covariance then the mean and covariance of the reconstructed image v can be calculated

$$\begin{aligned} \mu &= E[v] = \Omega\delta \\ \Sigma &= \mathrm{cov}(v) = \Omega\Gamma\Omega^T \end{aligned} \quad (3)$$

Where δ and Γ are the mean and covariance of the original vector f. Aside from the inverse Fourier transform, image processing techniques can also be represented as matrix operators. The same matrix representation in Eq. 2 can be used to complete reconstruction and processing [8].

$$v = Of \tag{4}$$

Where matrix O is the collection of matrix operators necessary to perform reconstruction and processing, f is a vector of observed values, and v is the reconstructed and processed complex-valued data. Again, if the original vector f has a known mean and covariance then the mean and covariance of the reconstructed image v can be calculated.

$$\begin{aligned} \mu &= E[v] = O\delta \\ \Sigma &= \mathrm{cov}(v) = O\Gamma O^T \\ \rho &= corr(v) = DO\Gamma O^T D \end{aligned} \tag{5}$$

Where δ and Γ are the mean and covariance of the original vector f, and D is a square matrix with diagonal elements formed by the reciprocal square root of the diagonal elements of $\mathrm{cov}(v)$.

ii. Registration

Registration is an extensive topic not only limited to medical imaging, a broad explanation is an image processing technique that aligns two or more images through geometric transformations. In fMRI, registration techniques are implemented for motion correction and spatial normalization [1,2].

The simplest and most common geometric transformation is completed using a rotation matrix with additional parameters. Rotation matrices are simple and linear, although non-linear methods that warp images exist as well such as thin plate splines [3,4]. Motion correction with rotation matrices consists of six parameters (6 degrees of freedom): three rotations about each axis, and three shifts along each axis. Spatial normalization consists of twelve parameters (12 degrees of freedom): three rotations about each axis, three shifts along each axis, three shears, and three

scales. Although these two registration techniques vary in number of parameters, the implementation remains the same for both.

The problem of registration can be described as the optimization of some cost function given the parameters [7]. The challenges of developing an algorithm for this problem are not just limited to accuracy but computational constraints as well. Due to the complexity of such an optimization problem, this project will only use 3 degrees of freedom (DOF). It is important to note that 3 DOF is insufficient for high quality image registration, especially inter-subject images, however a lower number of DOF will not affect the results of any induced correlation. Therefore, for this purposes of this project 3 DOF is sufficient.

iii. Interpolation

After the geometric transformation, an image has been rotated, shifted, sheared, and scaled the image intensity values and its corresponding may no longer be integer valued. Although the coordinates are Cartesian coordinates it is still necessary to convert to integers to correctly display 2-dimensional images [6]. Image interpolation methods are needed in order to make this correction. The majority of these methods attempt to interpolate new values based on some kind of distance weighting. Generally, sinc interpolation and trilinear interpolation is used but simpler methods are implemented in this project; this is done for the sake of computational efficiency, and the fact that these simpler methods create easier visualization. The interpolation methods used in this essay are nearest neighbor, mean weighted, bilinear, and inverse distance weighting.

(a) Nearest Neighbor	$z'_i = z(x_t, y_t),\ \min(\|\|(x_i, y_i) - (x_t, y_t)\|\|)$
(b) Mean	$z'_i = mean(z(x_t, y_t)),\ \|\|(x_i, y_i) - (x_t, y_t)\|\| < R$
(c) Bilinear	$z'_i = \sum_{t=1}^{4} w_{x_t, y_t} z_t(x_t, y_t)$

(d) Inverse Distance Weighted	$z'_i = \dfrac{\sum_{t=1}^{n} \dfrac{z_t}{\|(x_i, y_i)-(x_t, y_t)\|^p}}{\sum_{t=1}^{n} \dfrac{1}{\|(x_i, y_i)-(x_t, y_t)\|^p}}, \ \|(x_i, y_i)-(x_t, y_t)\| < R$

Table 1. (a) Where (x_i, y_i) is the location to be estimated, (x_i, y_i) is the location of known values, and z'_i is the interpolated image value. (b) Where (x_i, y_i) is the location to be estimated, (x_i, y_i) is the location of known values, z'_i is the interpolated image value, and R is some search radius. (c) Where (x_i, y_i) is the location of known values, and z'_i is the interpolated image value, and w_{x_t, y_t} is the weight. (d) Where p is the power, (x_i, y_i) is the location to be estimated, (x_i, y_i) is the location of known values, z'_i is the interpolated image value, and z_t is the known image values.

Using the same definitions and notations in Table 1, matrix operators can be formed to produce the same processing results. Each of the interpolation methods are creating weights with regards to distance between the interpolated point and the observed point; within the matrix operator, these weights first need to be calculated then place in the right location.

(a) Nearest Neighbor	$\begin{bmatrix} z'_1 \\ z'_2 \\ \vdots \\ z'_n \end{bmatrix} = \begin{bmatrix} w_{x_1,y_1} & 0 & \cdots & 0 & 0 \\ 0 & w_{x_2,y_2} & 0 & \cdots & 0 \\ & & & & \\ \vdots & & & \ddots & \\ 0 & & & & w_{x_n,y_n} \end{bmatrix} \begin{bmatrix} z_1 \\ z_2 \\ \vdots \\ z_n \end{bmatrix}, \ w = 1$
(b) Mean	$\begin{bmatrix} z'_1 \\ z'_2 \\ \vdots \\ z'_n \end{bmatrix} = \begin{bmatrix} w_1 & \cdots & w_1 & 0 & 0 \\ 0 & w_2 & \cdots & w_2 & 0 \\ & & & & \\ \vdots & & & \ddots & \\ 0 & & & & w_j \end{bmatrix} \begin{bmatrix} z_1 \\ z_2 \\ \vdots \\ z_n \end{bmatrix}, \ w_j = \dfrac{1}{n'}$
(c) Bilinear	$\begin{bmatrix} z'_1 \\ z'_2 \\ \vdots \\ z'_n \end{bmatrix} = \begin{bmatrix} w_{x_1,y_1} & \cdots & w_{x_4,y_4} & 0 & 0 \\ 0 & w_{x_1,y_1} & \cdots & w_{x_4,y_4} & 0 \\ & & & & \\ \vdots & & & \ddots & \\ 0 & & & & w_{x_1,y_1} \end{bmatrix} \begin{bmatrix} z_1 \\ z_2 \\ \vdots \\ z_n \end{bmatrix}$

(d) Inverse Distance Weighted	$\begin{bmatrix} z'_1 \\ z'_2 \\ \vdots \\ z'_n \end{bmatrix} = \begin{bmatrix} w_{1,1} & \cdots & w_{1,j} & 0 & 0 \\ 0 & w_{2,1} & \cdots & w_{2,j} & 0 \\ \vdots & & & \ddots & \\ 0 & & & & w_{n,1} \end{bmatrix} \begin{bmatrix} z_1 \\ z_2 \\ \vdots \\ z_n \end{bmatrix}, \; w_{i,j} = \frac{\frac{1}{\| (x_i, y_i) - (x_t, y_t) \|^p}}{\sum_{t=1}^{n} \frac{1}{\| (x_i, y_i) - (x_t, y_t) \|^p}}$

Table 2. Matrix operators of interpolation methods: (a) nearest neighbor, (b) mean, (c) bilinear, and (d) inverse distance weighted.

Given Eq. 2, if an image is $N \times N$ then a vector of image values f with both real and imaginary components would be $2N^2 \times 1$ and matrix operators of size $2N^2 \times 2N^2$. Since magnitude only images are used in this project, a vector of f would be $N^2 \times 1$ and matrix operators of size $N^2 \times N^2$. Although this can result in large matrices, the majority of the matrix operators are made up of zero values and sparse matrix representation is used to greatly improve computational efficiency. For example, a 4×4 image would have 16×16 matrix operators, Fig. 1 (a) – (d).

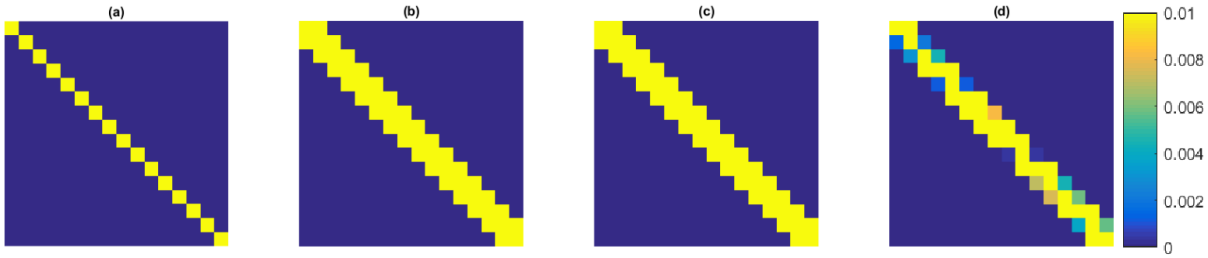

Figure 1. Example of 16×16 matrix operators, scaled to values between 0.0 and 0.01 to display non-zero values of operator. (a) nearest neighbor, (b) mean, (c) bilinear, (d) inverse distance weighted.

3. Methodology

Induced correlation from image processing can be quantified either with the use of simulation or matrix operators. It is easier to develop a simulation, but the use of matrix operators has greater accuracy and computational efficiency; both will be demonstrated and analyzed using magnitude data only. Although complex-valued data is collected and reconstructed, magnitude only data is used for its simplicity.

i. Function and Matrix Operator Accuracy

The simulation will use the functions defined in Table 1, whereas a real data set will be registered using the matrix operators defined in Table 2. The matrix operators need to provide the same results as their respective functions.

The accuracy of the matrix operators is best shown through an example. Using a single 96×96 Shepp–Logan phantom, normally distributed noise with mean, 0.0, and standard deviation, 0.1, is introduced to the image's intensity values and its respective coordinates centered about (0,0). Interpolation is required to grid the images to integer valued Cartesian coordinates; both functions and matrix operators are used for comparison, the results are displayed in Fig. 2 (a) – (d). The squared error between the two methods are computed and there are differences between the two but it is small enough to account to computer round off error. It is reasonable to conclude that the matrix operator will accomplish the same accuracy of interpolation as its respective functions.

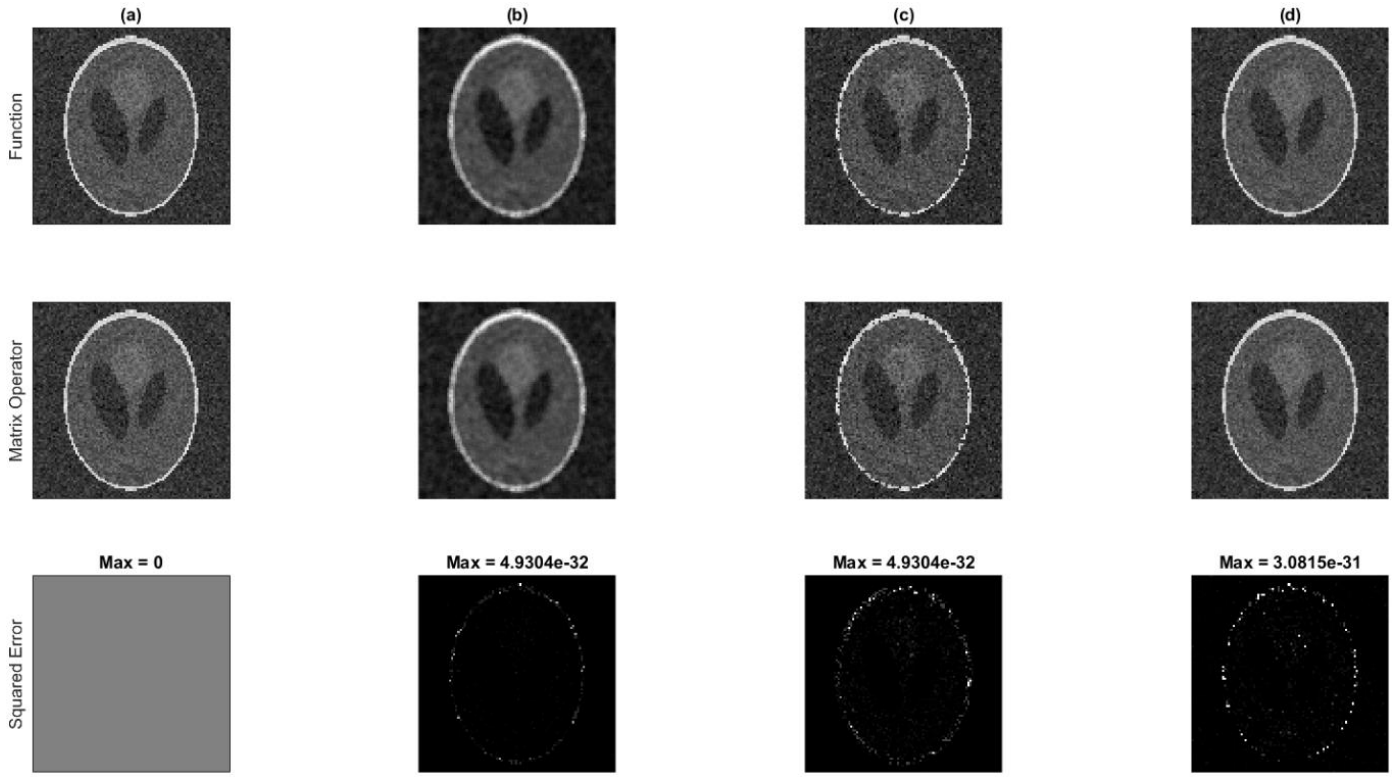

Figure 2. Comparison of interpolation results between function and matrix operator with max squared error. (a) nearest neighbor, (b) mean, (c) bilinear, (d) inverse distance weighted.

ii. Simulation

Images will have noise added to both the intensity values and their respective coordinates in order to simulate data that has already been geometrically transformed but still requires Cartesian grid interpolation. Using 100 samples of *96×96* Shepp – Logan phantoms, normally distributed noise with mean, 0.0, and standard deviation, 0.1, is introduced to the image's intensity values and its respective coordinates centered about (0,0). The simulation data will be interpolated using nearest neighbor, mean, bilinear, and inverse distance weighted defined in Table 1 (a) – (d). The parameter of the mean weighted interpolation is a search radius of three voxels. The parameters of the inverse distance weighted interpolation are a search radius of three voxels, and a power weighting of two.

iii. Matrix Operator

Using a data set where extreme motion is replicated where the subject periodically rotates their head. The data is collected from the General Electric 3.0 T Signa LX Magnetic Resonance Imager at the Medical College of Wisconsin. The single coil scan is composed of 11 slices with 720 time repetitions (TR) at 1 second each apart.

Motion correction will be performed on the first slice across 720 TR using the middle TR as the template by optimizing a geometric transformation with 3 DOF. After the optimization is completed, the scans will be interpolated using nearest neighbor, mean, bilinear, and inverse distance weighted matrix operators defined in Table 2 (a) – (d). The parameter of the mean weighted interpolation is a search radius of 3 voxels. The parameters of the inverse distance weighted interpolation are a search radius of 3 voxels, and a power weighting of 2.

4. Results

Using both simulation and matrix operators, the correlation between one voxel and every other voxel can be computed. The method and results between the two can be compared and analyzed.

i. Simulation

With 100 registered samples, covariance and correlation matrices can be computed. Each row of the covariance matrix is the covariance between one voxel and all others ordered by column, the diagonal elements of the covariance matrix is the variance of each voxel. Each column of the correlation matrix is the correlation between one voxel and all others ordered by row, the diagonal elements of the correlation matrix is equal to 1, Fig. 3 (a) – (d).

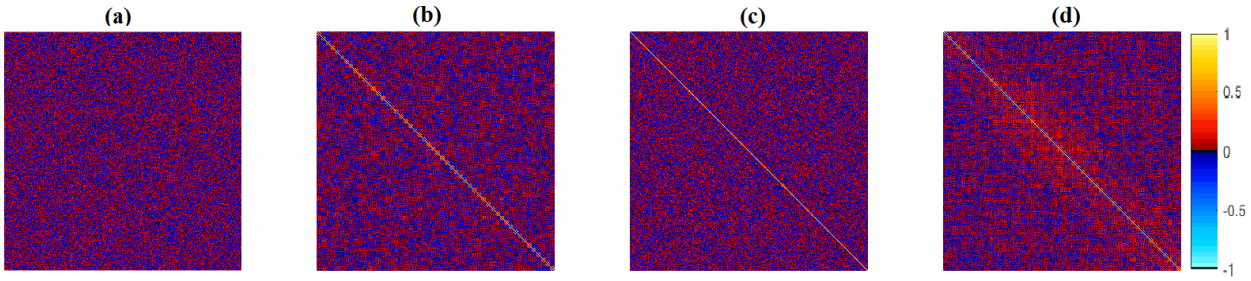

Figure 3. Correlation matrix computed from simulation of 100 registered images using (a) nearest neighbor, (b) mean, (c) bilinear, and (d) inverse distance weighted interpolation.

Each row of a correlation matrix is the correlation between voxel and all others. Each row can be reshaped, Fig. 4 (a) – (d), as well as overlayed the template image and passed through a threshold for better visualization, Fig. 5 (a) – (d).

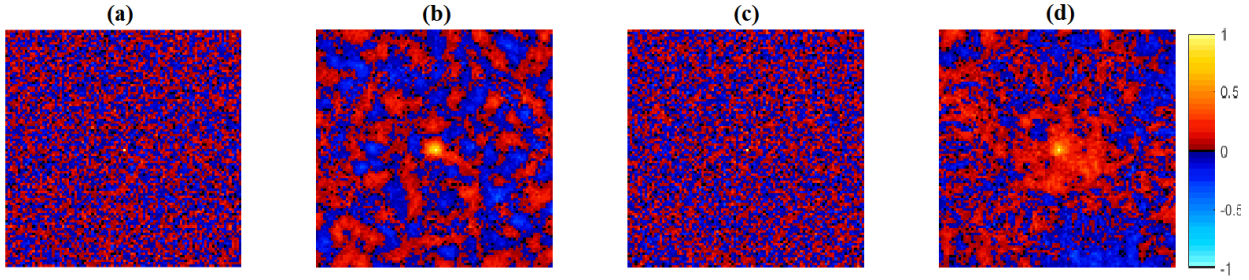

Figure 4. Correlation between center voxel and all others produced from simulation after (a) nearest neighbor, (b) mean, (c) bilinear, and (d) inverse distance weighted interpolation.

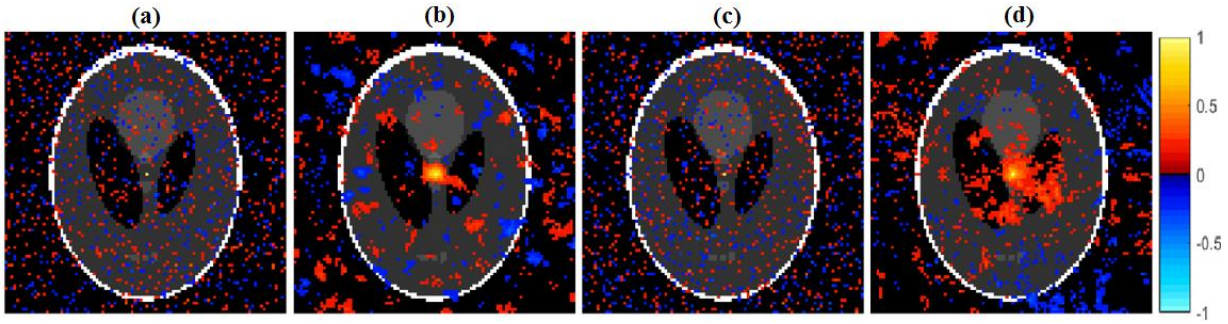

Figure 5. Correlation between center voxel and all others, overlayed the template image with a threshold value of 0.15 after (a) nearest neighbor, (b) mean, (c) bilinear, and (d) inverse distance weighted interpolation.

ii. Matrix Operator

With 720 optimizations performed, a correlation matrix is computed for each. As an example, the registration of TR = 720 to the template is examined, Fig. 6. (a) – (b). The optimization for this example is found to be a rotation of 13 degrees, a 1 voxel shift in the x-axis, and a 3 voxel shift in the y-axis.

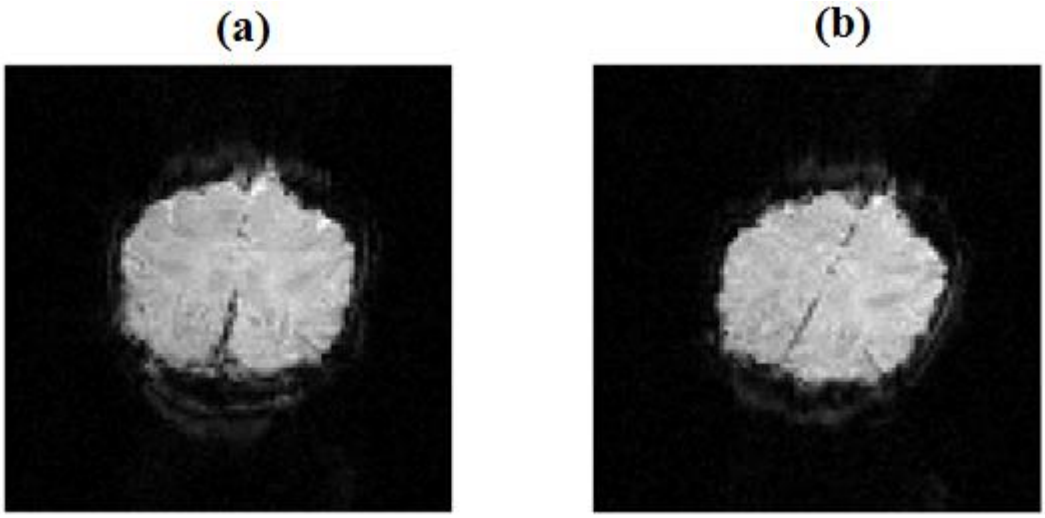

Figure 6. (a) Template image, and (b) slice 1, TR = 720.

Covariance and correlation matrices of the same structure can be computed. With the use of sparse matrix representation and the fact that simulations are not being computed makes matrix operators computationally superior, with respect to computation of covariance and correlation matrices.

Using matrix operators, the correlation matrices are computed; due to the large size of the correlation matrices it is difficult to display, instead only the first 1000×1000 elements are displayed in Fig. 7 (a) – (d).

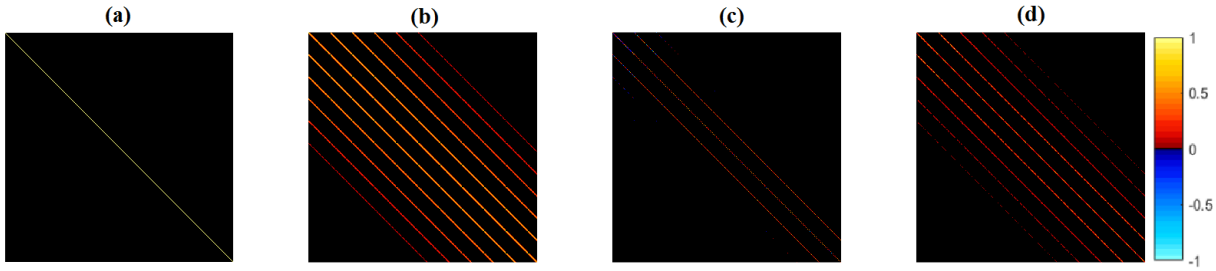

Figure 7. First 1000×1000 elements of correlations matrices computed from (a) nearest neighbor, (b) mean, (c) bilinear, and (d) inverse distance weighted.

Each row of a correlation matrix is the correlation between voxel and all others. Each reshaped, Fig. 8 (a) – (d), as well as overlayed the template image for better visualization, Fig. 9 (a) – (d).

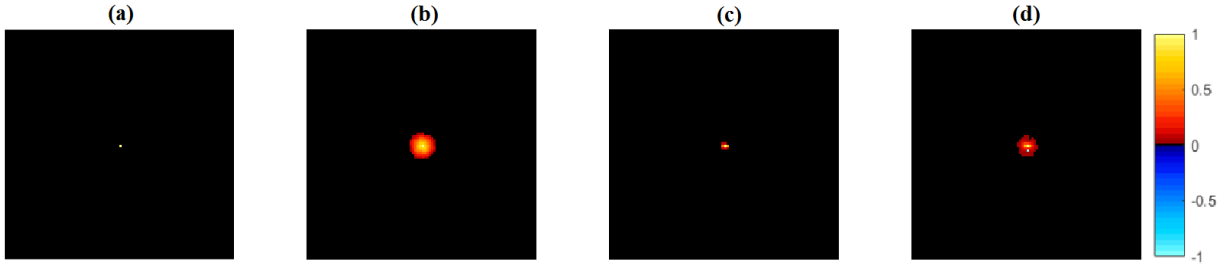

Figure 8. Correlation between center voxel and all others produced from matrix operators after (a) nearest neighbor, (b) mean, (c) bilinear, and (d) inverse distance weighted interpolation.

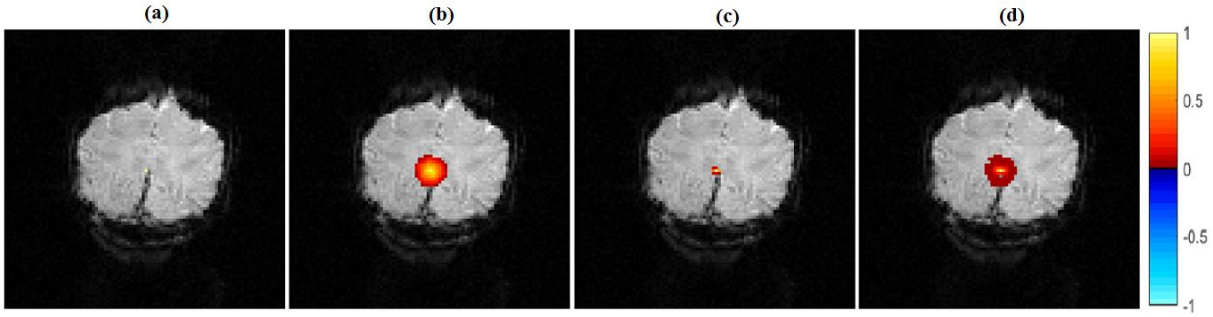

Figure 9. Correlation between center voxel and all others, overlayed the template image with a threshold value of 0.0001 after (a) nearest neighbor, (b) mean, (c) bilinear, and (d) inverse distance weighted interpolation.

iii. Comparison

When observing the center voxel's correlation with respect to all other voxels using the simulation results it is clear that some kind of correlation is present. However, it is unclear what the structure of the correlation is. With 100 samples, the noise included in the simulation is still indistinguishable from the induced correlation. As opposed to simulation, the use of matrix operators clearly defines the structure of the induced correlation.

With regards to the interpolation methods, nearest neighbor, mean, bilinear, and inverse distance weighted yield different results. Nearest neighbor interpolation does not induce correlation since it is simply a permutation matrix. Both mean and inverse distance weighted interpolation weight nearby values based on distance, creating a local radial correlation. Bilinear interpolation also weights with respect to is neighboring values, but only for the four closest neighboring values; this induces a very small local correlation, but it is not visible in the simulations due to scaling. At the least, the correlation computed from simulation reflects the results from matrix operators.

In these particular cases, the induced correlations are all local but that does not mean that far reaching correlations cannot be induced. This is most evident with the mean weighted and inverse distance weighted interpolation methods, the structure of the correlation is related to its respective parameters. When implementing mean weighted interpolation, if the search radius is increased then the size of the radially induced correlation also increases. When implementing inverse distance weighted interpolation, if the search radius is increased then the size of the radially induced correlation also increases, and if the power is increased the rate of change of the correlation increases. Any time some image processing method weights its neighboring values, induced correlation should be considered a possibility.

5. Conclusion

Image processing is an important step in fMRI analysis, the alignment of different images into the same coordinate plane allows for the computation of statistics. With the quantification of induced correlation due to image registration, at the very least researchers can be aware of the statistical effects. Linear matrix operator representations of these image processing techniques help theoretically visualize any induced correlation.

For future research, additional image processing techniques should also be examined. Sinc interpolation and trilinear interpolation are commonly used methods within registration packages and should be considered as well. The quantification of theoretical correlation also allows for the future research into models that account for the correlation

Bibliography

This work was supported by National Institutes of Health research grant R21NS087450.

[1] Ashburner, J., and K. Friston. "Rigid Body Registration". *Statistical Parametric Mapping* (2007): 49-62. Web. 13 Apr. 2016.

[2] Ashburner, John, and Karl J. Friston. "Nonlinear Spatial Normalization Using Basis Functions". *Human Brain Mapping* 7.4 (1999): 254-266. Web.

[3] Bookstein, F.L. "Principal Warps: Thin-Plate Splines And The Decomposition Of Deformations". *IEEE Transactions on Pattern Analysis and Machine Intelligence* 11.6 (1989): 567-585. Web. 13 Apr. 2016.

[4] Buhmann, M. D. *Radial Basis Functions*. Cambridge: Cambridge University Press, 2003. Print.

[5] Friston, Karl. J. et al. "Spatial Registration And Normalization Of Images". *Human Brain Mapping* 3.3 (1995): 165-189. Web. 13 Apr. 2016.

[6] Gianluca, Donato, and Serge Belongie. "Approximate Thin Plate Spline Mappings". *Proceedings of the 7th European Conference on Computer Vision-Part III (ECCV '02)* (2002): 21-31. Print.

[7] Jenkinson, Mark, and Stephen Smith. "A Global Optimisation Method For Robust Affine Registration Of Brain Images". *Medical Image Analysis* 5.2 (2001): 143-156. Web.

[8] Nencka, Andrew S., Andrew D. Hahn, and Daniel B. Rowe. "A Mathematical Model For Understanding The Statistical Effects Of K-Space (AMMUST-K) Preprocessing On Observed Voxel Measurements In Fcmri And Fmri". *Journal of Neuroscience Methods* 181.2 (2009): 268-282. Web. 13 Apr. 2016.

[9] Rowe, Daniel B., Andrew S. Nencka, and Raymond G. Hoffmann. "Signal And Noise Of Fourier Reconstructed Fmri Data". *Journal of Neuroscience Methods* 159.2 (2007): 361-369. Web. 13 Apr. 2016.

Marquette University

This is to certify that we have examined this copy of the essay by

Kevin K. Liu

And have found that it is complete and satisfactory in all respects.

This essay has been approved by:

_____

Dr. Daniel B. Rowe
Department of Mathematics, Statistics, and Computer Science

Approved on

_____